ORGANIC LETTERS

2012
Vol. 14, No. 9
2316–2319

Synthesis, Properties, and OFET Characteristics of 5,5′-Di(2-azulenyl)-2,2′-bithiophene (DAzBT) and 2,5-Di(2-azulenyl)-thieno[3,2-*b*]thiophene (DAzTT)

Yuji Yamaguchi, Yukihiro Maruya, Hiroshi Katagiri,* Ken-ichi Nakayama, and Yoshihiro Ohba

Graduate School of Science and Engineering, Yamagata University, 4-3-16 Jonan, Yonezawa, Yamagata 992-8510, Japan

kgri7078@yz.yamagata-u.ac.jp

Received March 22, 2012

ABSTRACT

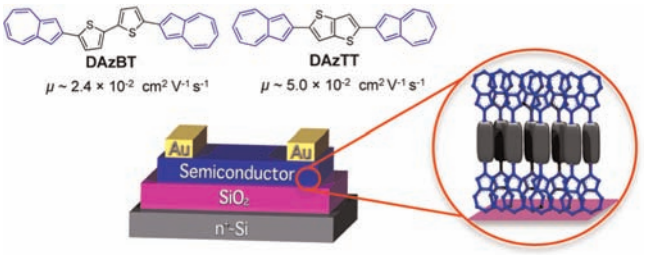

Two azulene-based π-conjugated systems, 5,5′-di(2-azulenyl)-2,2′-bithiophene and 2,5-di(2-azulenyl)-thieno[3,2-*b*]thiophene, were constructed via Suzuki−Miyaura cross-coupling reactions. The crystal structures of both revealed an edge-to-face orientation in a well-defined herringbone packing. The molecules stood nearly perpendicular to the substrate in the film form, with features of an organic field-effect transistor at hole mobilities of up to 5.0 $\times$ 10^{-2} cm^2 V^{-1} s^{-1}.

Flexible, thin, lightweight organic field-effect transistors (OFETs) have attracted attention for their potential uses in electronic devices, such as flexible displays, electronic paper, and radio frequency identification tags.[1] Various π-conjugated systems based on aromatic oligomers, such as benzene, naphthalene, thiophene, furan, and pyrrole, have been extensively studied in the past decade for their suitability as OFETs.[2] Azulene, an aromatic isomer of naphthalene, has an electrically positive seven-membered ring and an electrically negative five-membered ring, produces a large dipole moment of 1.0 D, and is bright blue owing to the small transition energy that arises from nonalternant polycyclic aromatic systems.[3] Recently, azulene-fused porphyrin[4] and azulenocyanine[5] have been reported as significantly expanded π-conjugation systems showing near-IR absorption, a high extinction coefficient, and a small HOMO−LUMO gap, which together make them suitable as semiconductors. As another recent example, azulene-based oligomers capable of effective optical band gap control and fluorescence switching have been reported.[6] Thus, azulene is an attractive candidate for the

(1) (a) Forrest, S. R. *Nature* **2004**, *428*, 911–918. (b) Arias, A. C.; MacKenzie, J. D.; McCulloch, I.; Rivnay, J.; Salleo, A. *Chem. Rev.* **2010**, *110*, 3–24. (c) Gelinck, G.; Heremans, P.; Nomoto, K.; Anthopoulos, T. D. *Adv. Mater.* **2010**, *22*, 3778–3798.

(2) (a) Facchetti, A. *Mater. Today* **2007**, *10*, 28. (b) Murphy, A. R.; Fréchet, J. M. J. *Chem. Rev.* **2007**, *107*, 1066–1096. (c) Katz, H. E.; Bao, Z. N.; Gilat, S. L. *Acc. Chem. Res.* **2001**, *34*, 359–369. (d) Miyata, Y.; Terayama, M.; Minari, T.; Nishinaga, T.; Nemoto, T.; Isoda, S.; Komatsu, K. *Chem.—Asian J.* **2007**, *2*, 1492–1504. (e) Fujii, M.; Nishinaga, T.; Iyoda, M. *Tetrahedron Lett.* **2009**, *50*, 555–558. (f) Nishinaga, T.; Miyata, T.; Tateno, M.; Koizumi, M.; Takase, M.; Iyoda, M.; Kobayashi, N.; Kunugi, Y. *J. Mater. Chem.* **2011**, *21*, 14959–14966.

(3) (a) Michl, J.; Thulstrup, E. W. *Tetrahedron* **1976**, *32*, 205–209. (b) Lemal, D. M.; Goldman, G. D. *J. Chem. Educ.* **1988**, *65*, 923–925.

(4) Kurotobi, K.; Kim, K. S.; Noh, S. B.; Kim, D.; Osuka, A. *Angew. Chem., Int. Ed.* **2006**, *45*, 3944–3947.

(5) Muranaka, A.; Yonehara, M.; Uchiyama, M. *J. Am. Chem. Soc.* **2010**, *132*, 7844–7845.

(6) Amir, E.; Amir, R. J.; Campos, L. M.; Hawker, C. J. *J. Am. Chem. Soc.* **2011**, *133*, 10046–10049.

(7) (a) Nozoe, T.; Seto, S.; Matsumura, S. *Bull. Chem. Soc. Jpn.* **1962**, *35*, 1990–1998. (b) Ito, S.; Nomura, A.; Morita, N.; Kabuto, C.; Kobayashi, H.; Maejima, S.; Fujimori, K.; Yasunami, M. *J. Org. Chem.* **2002**, *67*, 7295–7302.

10.1021/ol3007327
Published on Web 04/26/2012

construction of an effective π-conjugated system. To our knowledge, however, azulene derivatives have not yet been tested as OFETs.

Here we report the synthesis, properties, and OFET characteristics of 5,5′-di(2-azulenyl)-2,2′-bithiophene (**DAzBT**) and 2,5-di(2-azulenyl)-thieno[3,2-*b*]thiophene (**DAzTT**), in the first example of OFET materials based on π-conjugated azulene. In both compounds, the two azulenes are connected with the central bithiophene or thieo[3,2-*b*]thiophene unit at the 1,1′-position to permit the least steric hindrance between the five-membered rings, which reveal rectilinear and planar structures that form strong intermolecular interactions.

Scheme 1. Synthesis of 5,5′-di(2-azulenyl)-2,2′-bithiophene (**DAzBT**) and 2,5-di(2-azulenyl)-thieno[3,2-*b*]thiophene (**DAzTT**)

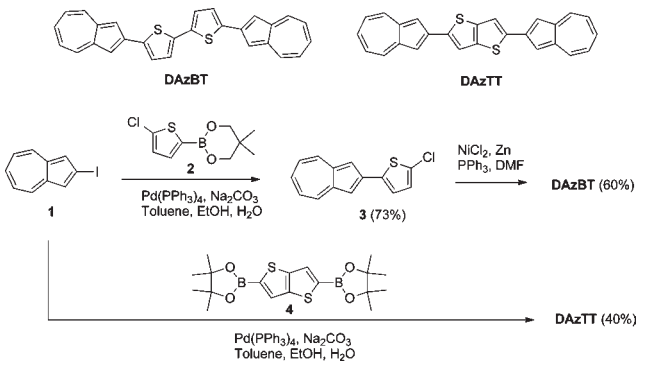

DAzBT was prepared in two steps from 2-iodoazulene **1** with 44% final yield and **DAzTT** in one step with 40% yield (Scheme 1). Since electrophilic substitution occurs at the "1" and "3" positions of the azulene ring, 2-iodoazulene **1** cannot be obtained directly from azulene and was therefore prepared from cyclopentadiene in seven steps via tropolone derivatives.[7] For the preparation of **DAzBT**, **1** was reacted with 5-chlorothiophene-2-boronic acid pinacol ester **2**[8] by Pd[PPh_3]$_4$-catalyzed Suzuki–Miyaura cross-coupling reaction to give 2-(2-azulenyl)-5-chlorothiophene **3**; this was subjected to a nickel–phosphine complex-catalyzed homocoupling reaction to give **DAzBT** as dark-green crystals. For the preparation of **DAzTT**, Suzuki–Miyaura cross-coupling of **1** with thienothiophene diboronic acid ester **4**[9] proceeded readily to give **DAzTT** as dark-green crystals. These compounds were purified by gradient sublimation and characterized by elemental analysis and single-crystal X-ray diffraction.

Single crystals of **DAzBT** and **DAzTT** grown by slow gradient sublimation had almost planar forms and similar packing formation (Figures 1a, 2a). The maximum deviations from the mean plane were ca. 0.17 Å for **DAzBT** and 0.20 Å for **DAzTT**.[10] The molecular long axes (*c* axes) exhibited a layer structure in both crystals (Figures 1b and 2b), which took the form of well-defined herringbone packing structures typical of edge-to-face stacking (Figures 1c, 2c). Although both crystals showed interatomic contacts, those in **DAzBT** were based on carbon···carbon contacts and 1D columnar interaction, while those in **DAzTT** were based on sulfur···carbon contacts and 2D planar interatomic contacts. PLATON/VOID[11] software calculated packing coefficients of 73.8% in **DAzTT** and 73.1% in **DAzBT**.

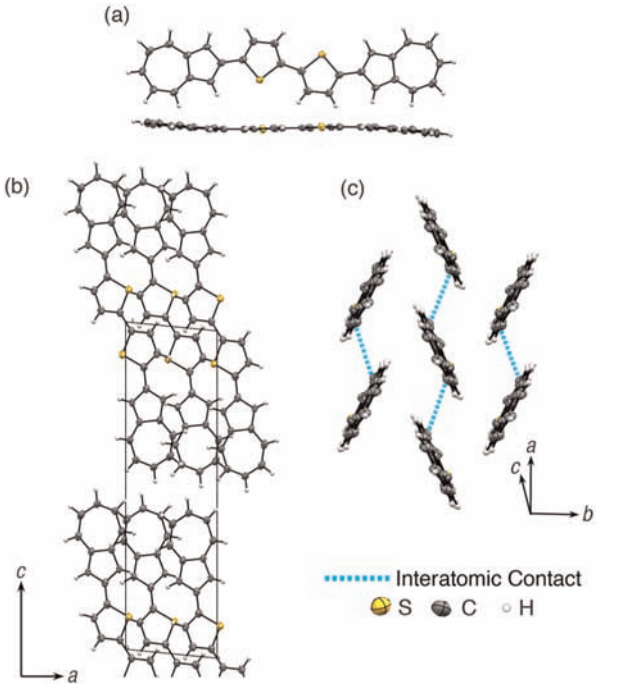

Figure 1. Crystal structure of **DAzBT**. (a) Thermal ellipsoid drawing of top and side views at 50% probability level. (b) Partial view along the *b* axis with clear indication of a layer structure along the *c* axis. (c) Perspective view with clear indication of the herringbone packing and the 1D columnar interatomic contacts.

(8) Ebdrup, S.; Jacobsen, P.; Farrington, A, D.; Vedsø, P. *Bioorg. Med. Chem.* **2005**, *13*, 2305–2312.

(9) Tang, W.; Singh, S. P.; Ong, K. H.; Chen, Z. K. *J. Mater. Chem.* **2010**, *20*, 1497–1505.

(10) L.S. planes were calculated through the all nonhydrogen atoms with PLATON program; see ref 11.

(11) Spek, A. L. *J. Appl. Crystallogr.* **2003**, *36*, 7–13.

(12) Tian, H.; Shi, J.; He, B.; Hu, N.; Dong, S.; Yan, D.; Zhang, J.; Geng, Y.; Wang, F. *Adv. Funct. Mater.* **2007**, *17*, 1940–1951.

(13) Cornil, J.; Beljonne, D.; Calbert, J. P.; Brédas, J. L. *Adv. Mater.* **2001**, *13*, 1053–1067.

(14) Mattheus, C. C.; de Wijs, G. A.; de Groot, R. A.; Palstra, T. T. M. *J. Am. Chem. Soc.* **2003**, *125*, 6323–6330.

(15) Marseglia, E. A.; Grepioni, F.; Tedesco, E.; Braga, D. *Mol. Cryst. Liq. Cryst.* **2000**, *348*, 137–151.

(16) (a) Ebata, H.; Izawa, T.; Miyazaki, E.; Takimiya, K.; Ikeda, M.; Kuwabara, H.; Yui, T. *J. Am. Chem. Soc.* **2007**, *129*, 15732–15733. (b) Yamamoto, T.; Takimiya, K. *J. Am. Chem. Soc.* **2007**, *129*, 2224–2225. (c) Takimiya, K.; Shinamura, S.; Osaka, I.; Miyazaki, E. *Adv. Mater.* **2011**, *23*, 4347–4370.

(17) DFT calculations were carried out with Gaussian 09 program package: Frisch, M. J. et al. *Gaussian 09*, revision C.01; Gaussian, Inc.: Wallingford, CT, 2010; see Supporting Information for full reference.

(18) Tian, H.; Shi, J.; Dong, S.; Yan, D.; Wang, L.; Geng, Y.; Wang, F. *Chem. Commun.* **2006**, 3498–3500.

(19) Nicolas, Y.; Blanchard, P.; Roncali, J.; Allain, M.; Mercier, N.; Deman, A.-L.; Tardy, J. *Org. Lett.* **2005**, *7*, 3513–3516.

(20) Merlo, J. A.; Newman, C. R.; Gerlach, C. P.; Kelley, T. W.; Muyres, D. V.; Fritz, S. E.; Toney, M. F.; Frisbie, C. D. *J. Am. Chem. Soc.* **2005**, *127*, 3997–4009.

These results together indicate that the sulfur atoms take a more effective role in the packing structure of **DAzTT**. Interestingly, the C···C distance in **DAzBT** is shorter than that in 5,5′-bis(naphth-2-yl)-2,2′-bithiophene,[12] which means that the azulene unit has a higher packing efficiency than the naphthalene unit despite the antiparallel stackable feature of azulene units due to their polarized structure. These herringbone characteristics are generally observed in high-mobility OFET materials, such as pentacene,[13,14] oligothiophene,[13,15] and various thienoacenes.[16]

The UV−vis spectra of the azulene oligomers in film form showed absorption maxima (λ_{max}) of around 630 and 690 nm (in the visible region) for both (Table 1, Figure 3). The lowest transition energies ($E_{g\text{-}abs}$) estimated from the absorption edges and the ionization potential (IP) determined by photoelectron yield spectroscopy of **DAzBT** and **DAzTT** were similar. The IP values were −5.43 and −5.45 eV (Table 1), showing good positioning with respect to the Fermi level of a gold electrode (−4.9 eV). Both compounds had small transition energies (1.74 eV), and these values were close to that of unsubstituted azulene (1.8 eV),[3a] indicating that the characteristic transitions of the longest absorption band for **DAzBT** and **DAzTT** are considered to be similar to that for unsubstituted azulene. The lowest transition energies calculated by the time-dependent density functional theory (TD-DFT) method[17] were both 2.27 eV, with contributions of HOMO−2 to LUMO excitation (CI coefficient = 0.59) in **DAzBT**, HOMO−1 to LUMO excitation (0.63) in **DAzTT**, and HOMO to LUMO excitation in **DAzBT** (0.18) and **DAzTT** (0.10) (Figure S9 in Supporting Information). Thus the transition energy of these molecules probably cannot be treated as a simple HOMO−LUMO transition as seen in a number of π-conjugated molecules.

We fabricated OFET devices by vacuum deposition in a top-contact type of configuration with an active layer thickness of 60 nm on bare Si/SiO_2 substrate or hexamethyldisilazane (HMDS)-treated Si/SiO_2 substrate (Table 2). Both devices gave typical p-channel responses and good saturation behaviors in the output curves (Figure 4a,c). A **DAzTT**-based device fabricated on HMDS-treated Si/SiO_2 gave the best OFET performance, with a carrier mobility (μ_{FET}) of 5.0×10^{-2} cm^2 V^{-1} s^{-1}, on/off ratios (I_{on}/I_{off}) of 1.1×10^5, and a threshold voltage (V_{Th}) of −5 V. HMDS treatment had little effect on μ_{FET} performance but decreased V_{Th}. Overall, the mobilities of **DAzTT** were higher than those of **DAzBT** on account of the more effective intermolecular interaction in the **DAzTT** crystals (see above). The FET performance of **DAzBT** was comparable to other similar materials using, such as naphthalene,[12] phenanthrene,[18] benzothiophene,[12] or naphthothiophene[19] as the end-capping unit. Higher μ_{FET} has been reported when employing larger linear acenes, anthracene, and tetracene.[20]

X-ray diffraction measurements with an out-of-plane configuration of **DAzBT** and **DAzTT** on HMDS-treated Si/SiO_2 gave a series of peaks assignable to (00h) reflections (Figure 5). The diffraction peak at $2\theta = 4.04°$ corresponds to a d-spacing of 21.9 Å for **DAzBT**, and that at $2\theta = 4.32°$ corresponds to a d-spacing of 20.4 Å for **DAzTT**, in good agreement with the c axis lengths of the single crystals, respectively, 21.6 and 20.0 Å (Figures 1b, 2b). These results

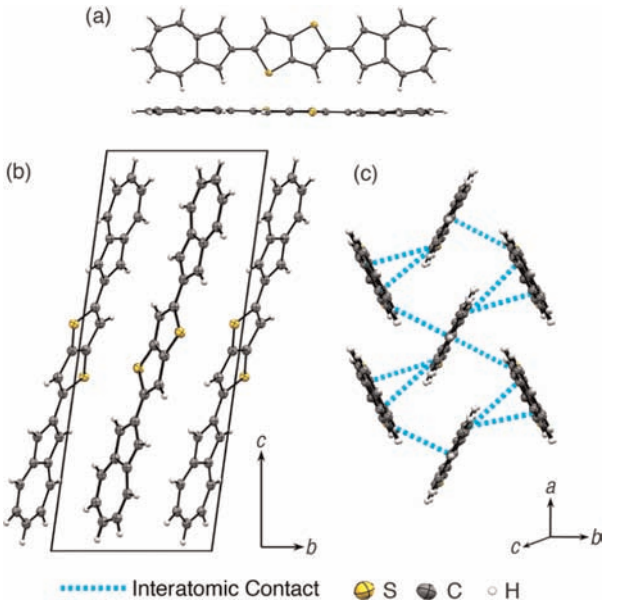

Figure 2. Crystal structure of **DAzTT**. (a) Thermal ellipsoid drawing of top and side views at 50% probability level. (b) Partial view along the a axis with clear indication of a layer structure along the c axis. (c) Perspective view with clear indication of the herringbone packing and the 2D planar interatomic contacts.

Table 1. UV−vis and PYS Data of **DAzBT** and **DAzTT**

compound	λ_{max}[a] (nm)	λ_{onset} (nm)	$E_{g\text{-}abs}$[b] (eV)	IP[c] (eV)
DAzBT	630, 688	712	1.74	−5.43
DAzTT	629, 689	714	1.74	−5.45

[a] Absorption spectra in thin film forms. [b] Determined from the absorption edge. [c] Determined by photoemission yield spectroscopy (PYS).

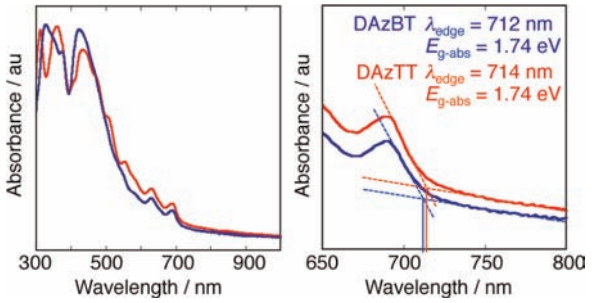

Figure 3. UV−vis spectra of **DAzBT** (blue) and **DAzTT** (red) in thin-film form. The lowest transition energies ($E_{g\text{-}abs}$) were determined from the intersection of the line tangent to the long wavelength side of the band and the corrected baseline.

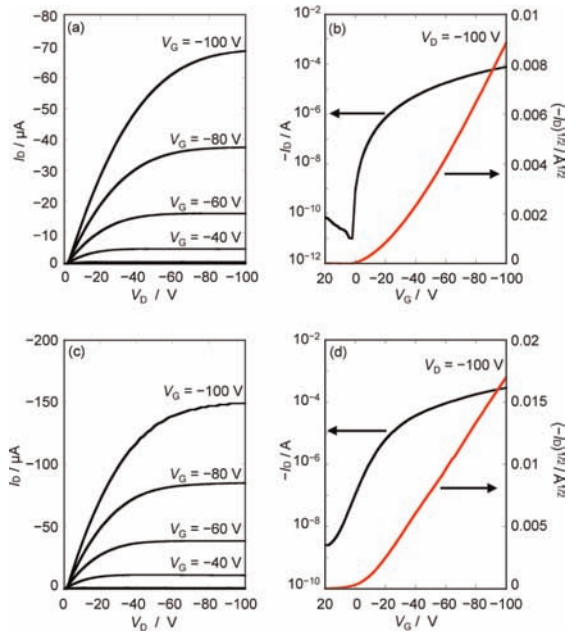

Figure 4. OFET characteristics of top-contact devices made of (a,b) **DAzBT** and (c,d) **DAzTT** at ambient temperature. (a,c) Output curves at different gate voltages. (b,d) Transfer curves in the saturated region at a drain voltage of −100 V.

Table 2. OFET Characteristics of **DAzBT** and **DAzTT**

compound	surface treatment	T_{sub}[a]	μ_{FET} ($cm^2 V^{-1} s^{-1}$)	I_{on}/I_{off}	V_{Th} (V)
DAzBT	bare	rt	2.4×10^{-2}	1.7×10^{6}	−25
	HMDS	rt	1.8×10^{-2}	8.0×10^{6}	−18
DAzTT	bare	rt	4.7×10^{-2}	1.3×10^{5}	−12
	HMDS	rt	5.0×10^{-2}	1.1×10^{5}	−5

[a] rt = room temperature.

show that the molecules stood nearly perpendicular to the substrate (edge-on orientation) in the film form. On the other hand, weak peaks were assignable to (111) in **DAzBT** and to (1−11) in **DAzTT**, indicating a coexisting face-on orientation (Figure 5b). Although out-of-plane X-ray diffraction showed high-ordered structures in thin films of both **DAzBT** and **DAzTT**, the packing advantage of the 2D network interatomic contacts in **DAzTT** is one reason why μ_{FET} was higher in **DAzTT** (Table 2). Thin-film morphology revealed by atomic force microscopy showed crystal growth with small grains that seem to be rough with high crystallinity (Figure S11, Supporting Information).

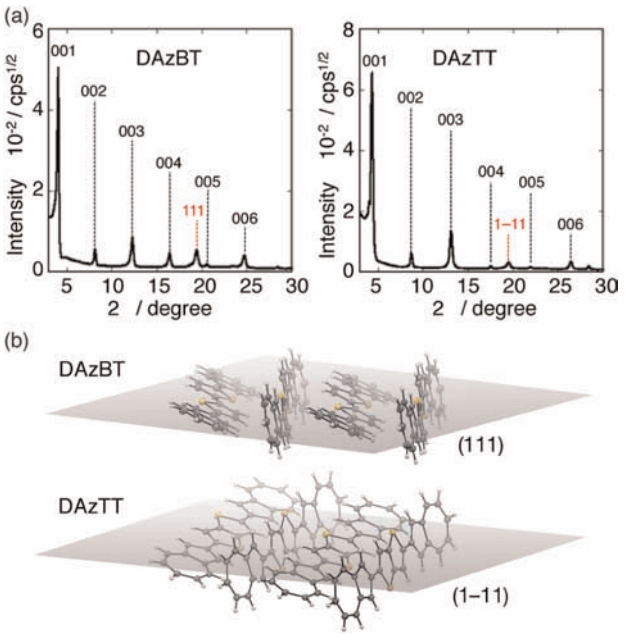

Figure 5. (a) Out-of-plane X-ray diffraction patterns of evaporated thin films of (left) **DAzBT** and (right) **DAzTT** on HMDS-treated Si/SiO_2 substrate. (b) Single-crystal X-ray structure of (upper) **DAzBT** and (lower) **DAzTT** with clear indication of their face-on orientations.

In general, azulene is less stable than naphthalene.[3b] Thermogravimetric analysis under flowing nitrogen showed good thermal stability of both compounds: onset of decomposition at 432 °C for **DAzBT** and 430 °C for **DAzTT** (Figure S12, Supporting Information).

We have synthesized novel azulene-based oligomers and used π-conjugation to create OFETs. These compounds showed small transition energies due to their effective π-conjugation system, high-order orientations in the crystalline state, and typical p-channel OFET characteristics with comparatively high carrier mobilities. We are now working on optimizing their carrier mobilities and investigating materials based on this molecular design.

Acknowledgment. This work was supported by a Grant-in-Aid for Young Scientist (B) (19750104 to H.K.) from the Ministry of Education, Culture, Sports, Science and Technology (MEXT).

Supporting Information Available. Experimental details and ^1H and ^{13}C NMR spectra. This material is available free of charge via the Internet at http://pubs.acs.org.

The authors declare no competing financial interest.